International Journal of Technology 14(2) 330-338 (2023)
Received November 2020 / Revised March 2021 / Accepted May 2022

International Journal of Technology

The Formation Process of Hydroxyapatite Nanoparticles by Electrolysis and Their Physical Characteristics

Supriyono[1*], Christina Wahyu Kartikowati[1**], Bambang Poerwadi[1], Chindy Wulandari[1], Lyla Liilia Fitria Hikma[1], Aulia Azzahra[1], Kharisma Ghanyysyafira[1], Hira Listya Pinastika[1]

[1]*Chemical Engineering Department, Faculty of Engineering, Universitas Brawijaya, Jl. MT. Haryono No. 167, Malang 65145, Indonesia*

Abstract. The electrolysis method for synthesizing hydroxyapatite nanoparticles (NPs) has the advantage of controlling the particle size by adjusting the potential and current used. This study aims to study the electrolysis of hydroxyapatite NPs formation and its characteristics. The solution contained $Na_2H_2EDTA.2H_2O$, KH_2PO_4, and $CaCl_2$, with an $EDTA/PO_4^{3-}/Ca^{2+}$ concentration of 0.2/0.2/0.2 M. The electrolytic potential are 4, 5, and 6 volts for 6 hours. The carbon electrode spacing used is 2 cm. The precipitate formed is filtered with a vacuum jet ejector. Retentate was washed with demineralized water and dried in an oven at 105˚C. The synthesis of pure hydroxyapatite by electrolysis was successfully carried out at a potential of 5 volts. The OH^- ion, which comes from the H_2O reduction process at the cathode, is essential in the formation of brushite, which then forms hydroxyapatite. The hydroxyapatite, synthesized at a potential of 4 volts, had the smallest particle size (442.4 nm) with the largest particle surface area (417.22 m^2/gram).

Keywords: Bioceramics; Electrolysis; Hydroxyapatite; Nanoparticles

1. Introduction

Hydroxyapatite (HA) particles are a biomaterial having a chemical formula of $Ca_{10}(PO_4)_6(OH)_2$. HA has good biocompatibility and bioactivity properties. The structure of HA approximates the structure possessed by bones and teeth (Pietrzykowska *et al.*, 2021; Tomozawa and Hiromoto, 2011; Suchanek and Yoshimura, 1998). HA can bind directly to tissue and stimulate tissue growth. Therefore, HA has the potential to be applied in the biomedical field, especially for bone and dental applications (Zhou and Lee, 2011).

HA belongs to the bioceramic type. In the medical world, ceramic materials are divided into two groups, namely bioinert ceramics and bioactive ceramics. Bioinert ceramics have no effect and interact with body tissues (Panda, Biswas, and Paul, 2021). Meanwhile, bioactive ceramics can bind to living bone tissue, such as HA and calcium phosphate. HA can be used in a variety of biomedical applications, including matrices for drug release control (Kamitakahara, Imai, and Ioku, 2013), scaffolds for new bone formation (Rezwan *et al.*, 2006), and fillers and coatings for repairing osseous damage (Zhou and Lee, 2011; Banerjee,

*Corresponding author's email: supriyono16@ub.ac.id, Tel.: +62-341-587710; Fax.: +62-341-574140
**Corresponding author's email: christinawahyu@ub.ac.id, Tel.: +62-341-587710; Fax.: +62-341-574140
doi: 10.14716/ijtech.v14i2.4452

Bandyopadhyay, and Bose, 2007). In the biomedical field, nano-sized HA particles have better bioactivity than micro-particles (Dorozhkin, 2010).

Various methods have been developed to synthesize HA NPs, including precipitation, hydrothermal, mechano-chemical, flame spray, and electrolysis (Córdova-Udaeta *et al*., 2021; Lin *et al*., 2017; Martins *et al*., 2008; Fathi and Hanifi, 2007; Chang and Tanaka, 2002). Djosic *et al.* (2009) have succeeded in synthesizing monetite nanoparticles electrochemically and transforming them into hydroxyapatite by immersion in NaOH solution. However, no research has been conducted on the conditions affecting the electrochemical process to produce hydroxyapatite directly (one step) (Djosic *et al*., 2009). Electrolysis is a method that offers an easy and straightforward process (Corona-Gomez, Chen, and Yang, 2016). The particle diameter can be controlled by adjusting the voltage or current during electrolysis (Djosic *et al*., 2009). These results were obtained from tests with relatively high solution pH and current density. Theoretically, the higher the pH and current density will accelerate the particle formation reaction and encourage particle agglomeration (Kim, Kim, and Hirasawa, 2002). If the pH and current density are relatively high, the pH and current density no longer affect the particle size but are more influenced by the number of reactants available and the synthesis time. At relatively low current densities, these two parameters may have an effect (Montero *et al*., 2006). Therefore, this research focuses on studying the operating conditions, namely the potential for synthesizing hydroxyapatite NPs.

2. Methods

2.1. Materials and Instrumentations

The raw materials used in this study include $Na_2H_2EDTA.2H_2O$ (Merck), KH_2PO_4 (Merck), $CaCl_2.7H_2O$ (Merck), and commercial hydroxyapatite (Merck). While the instrumentation used includes a DC power supply (GPD X303S, GW Instek), Particle Size Analyzer (Cilas 1190), Surface Area Analyzer (Quantachrome NOVA 1200), and Powder X-ray Diffraction (PANalytical X'Pert3 Powder).

2.2. Synthesis of Hydroxyapatite NPs Powder

HA NPs powder was prepared by electrolysis method. The arrangement of the tools in the experiment for the synthesis of HA NPs is shown in Figure 1. The series of tools consists of a set of electrolysis cells consisting of 2 carbon electrodes of 10 cm x 4 cm x 0.7 cm each as an anode and cathode and a DC power supply. The electrolyte solution consisted of 133 mL of $Na_2H2EDTA.2H_2O$, KH_2PO_4, and $CaCl_2$ with a concentration of $EDTA/PO_4^{3-}/ Ca^{2+}$ of 0.2/0.2/0.2 M. The electrolysis cell is connected to a DC power supply providing a potential difference between the two electrodes. The electrolytic potential are 4, 5, and 6 volts for 6 hours. The precipitate formed is filtered with a vacuum jet ejector. Retentates were washed with demineralized water and dried in an oven at 105˚C until constant weight. Furthermore, characterization of synthesized particle products by electrolysis. The XRD (X-Ray Diffraction) method was used to determine the causative purity of the synthesized particles by electrolysis. The PSA (Particle Size Analyzer) method was used to measure the distribution and particle size. Meanwhile, to determine the surface area of biochar, the Quantachrome NOVA 1200 was used.

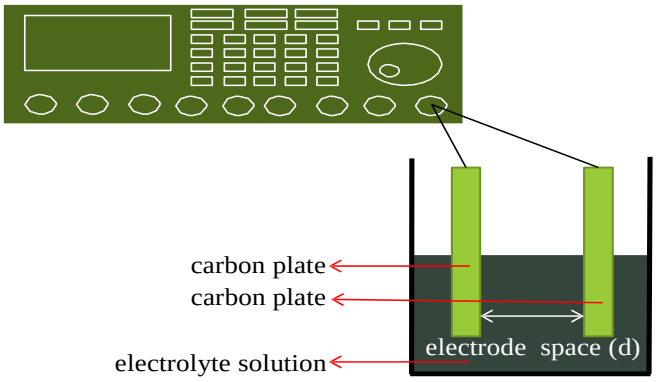

Figure 1 Schematic diagram of electrolysis for synthesizing HA NPs

3. Results and Discussion

3.1. Synthesis of Hydroxyapatite NPs

Figure 2 shows the synthesized white powder's X-ray diffraction pattern (XRD). The synthesized white powder shows a tendency to form hydroxyapatite NPs which is consistent with the peak position at an angle of 2θ with JCPDS 03-0747, hexagonal, a = b = 9.4302, c = 6.88911 Å, space group P63/m. Referring to the reaction, the formation of hydroxyapatite NPs occurs reversibly; the synthesis of hydroxyapatite NPs requires an optimal reaction equilibrium (Nur *et al.*, 2014). If the electrolysis voltage during the hydroxyapatite NPs formation process is set to the correct value, then the reaction tends to lead to the formation of hydroxyapatite NPs.

The white powder synthesized from bulk solution at potential 4 Volt has a mixture composition of brushite and hydroxyapatite NPs. The lack of energy used resulted in converting the brushite to hydroxyapatite NPs. The white powder synthesized from bulk solution at a potential of 5 Volts has a pure hydroxyapatite NPs composition. Meanwhile, the white powder which was synthesized from bulk solution at a potential of 6 volts had a dominant composition of hydroxyapatite NPs with a small amount of brushite. This is because the reaction to form hydroxyapatite from brushite is a back-and-forth reaction (Tripathi and Basu, 2012). If the hydroxyapatite NPs still contain brushite, it will reduce their bioactivity when applied medically (Dorozhkin, 2010). The hydroxyapatite formed also has a tendency with the amorphous phase.

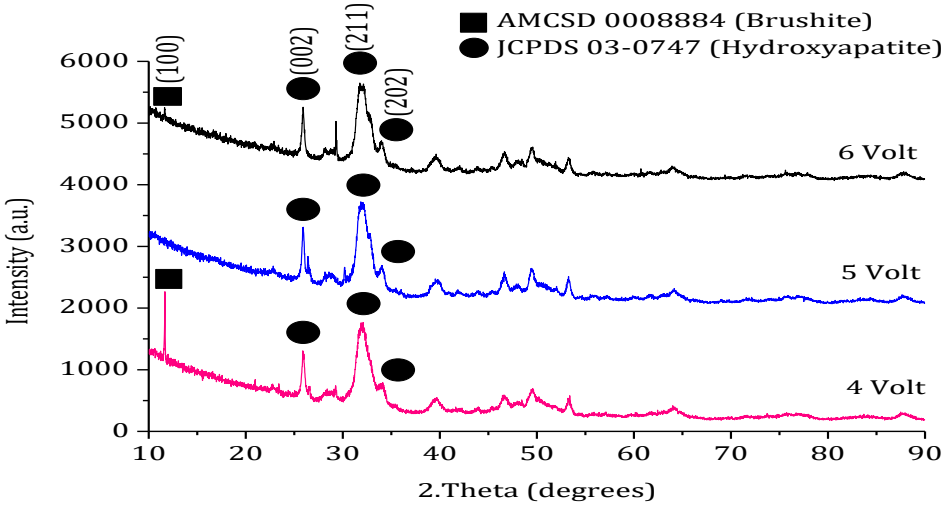

Figure 2 The X-ray diffraction pattern of the synthesized white powder by electrolysis

3.2. Reaction Mechanism for the Formation of Hydroxyapatite NPs

The reaction mechanism of the formation of hydroxyapatite NPs can be explained by several possible reactions. Figure 3 shows a schematic diagram of the reaction mechanism for forming hydroxyapatite NPs. The water reduction reaction at the cathode that produces OH^- ions are in accordance with the following reaction 1:

$$2H_2O + 2e^- \rightarrow 2OH^- + H_2 \quad (1)$$

After the reduction of water at the cathode producing OH^- ions. The produced OH^- ions induce an acid-base reaction to form PO_4^{3-} and HPO_4^{2-} with the following reactions 2 and 3,

$$H_2PO_4^- \rightarrow HPO_4^{2-} + H^+ \quad (2)$$
$$HPO_4^{2-} \rightarrow PO_4^{3-} + H^+ \quad (3)$$

This reaction was expected to affect the composition of calcium phosphate ultimately determining whether the apatite phase is in the form of HA or brushite (Montero *et al*., 2006). This reaction is greatly influenced by the OH- ions' formation rate. If the OH^- ion formation rate is slower than the minimum required amount, HPO_4^{2-} becomes stable and tends to form brushite ($CaHPO_4.2H_2O$). When the rate of OH^- formation is faster than the minimum required amount of OH^-, the PO_4^{3-} becomes more stable than HPO_4^{2-}, which encourages the formation of HA (Montero *et al*., 2006). Calcium phosphate precipitates are formed with all the reactants needed for the formation of Ca-P bonds (Ca^{2+}, PO_4^{3-}, HPO_4^{2-}, and OH^-) with the following reaction 4,

$$5Ca^{2+} + 3\ PO_4^{3-} + OH^- \rightarrow Ca_5(PO_4)_3(OH) \quad (4)$$

Another factor in controlling the formation of calcium phosphate is the concentration of Ca^{2+} ions (Nasiri-Tabrizi *et al*., 2009). Controlling the Ca^{2+} concentration is carried out by using an EDTA stabilizer to prevent the rapid precipitation of calcium phosphate, which is expected to affect the size of the particles formed as indicated by the following reaction 5,

$$Ca(EDTA)^{2-} \leftrightarrow Ca^{2+} + EDTA^{4-} \quad (5)$$

The total reaction of the formation of HA become

$$10\ Ca^{2+} + 6\ PO_4^{3-} + 2\ OH^- \leftrightarrow Ca_{10}(PO4)_6(OH)_2 \quad (6)$$

Hydroxyapatite ($Ca_{10}(PO_4)_6(OH)_2$) NPs formed is indicated by the presence of white deposits in the area around the cathode.

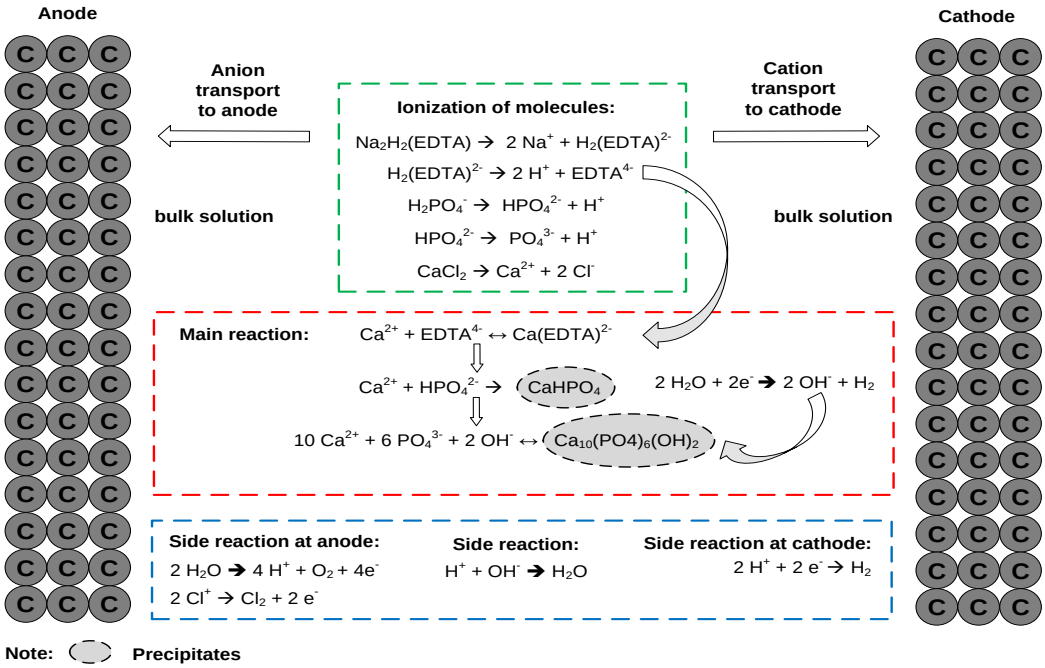

Figure 3 Schematic diagram of the reaction to the electrolytic formation of hydroxyapatite

Figure 4 shows the process of hydroxyapatite formation characterized by a change in the color of the bulk solution. The yellow indicates $Ca(EDTA)^{2-}$ (Xin, Ren and Leng, 2010). The $Ca(EDTA)^{2-}$ ions began to form significantly at the time of synthesis to 300 minutes. Hydroxyapatite powder was formed in the cathode area, which was indicated by deposited white powder.

0 minute 60 minutes 120 minutes 180 minutes

240 minutes 300 minutes 360 minutes

Figure 4 Photo of color change with time of electrolysis of hydroxyapatite NPs by electrolysis

3.3. Distribution of Hydroxyapatite Nanoparticles Diameter

The hydroxyapatite NPs were synthesized by electrolysis at a potential of 4, 5, and 6 Volts, which were tested for the particle diameter distribution using the PSA method. The results of the PSA analysis are shown in Figure 5. Figure 5 shows that the hydroxyapatite NPs generated from electrolysis at a potential of 4 volts have the smallest average particle diameter of 442.4 nm. While the particles resulting from electrolysis at a potential of 5 Volts and 6 Volts have an average particle diameter of 843.1 nm and 1519 nm, respectively. This is because the particles produced from electrolysis at a potential greater than 4 volts have a tendency to agglomerate, forming particles of a larger size.

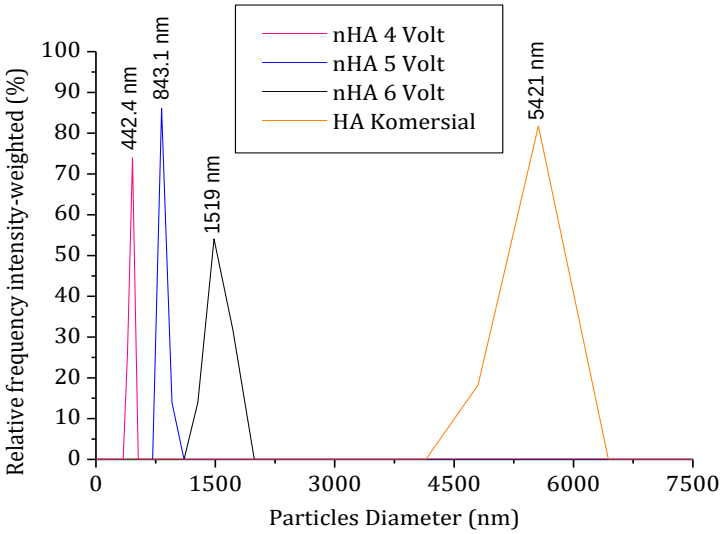

Figure 5 Size distribution of as-synthesized HA NPs by electrolysis and commercial HA

The synthesized hydroxyapatite NPs have a smaller particle size than commercial hydroxyapatite particles (5421 nm). This is due to the lack of pushing force of H_2 gas to the outside, formed from the H_2O reduction reaction around the cathode, as described in the mechanism for forming hydroxyapatite NPs in Figure 6.

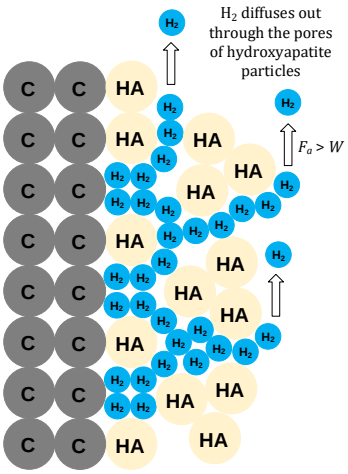

(a)

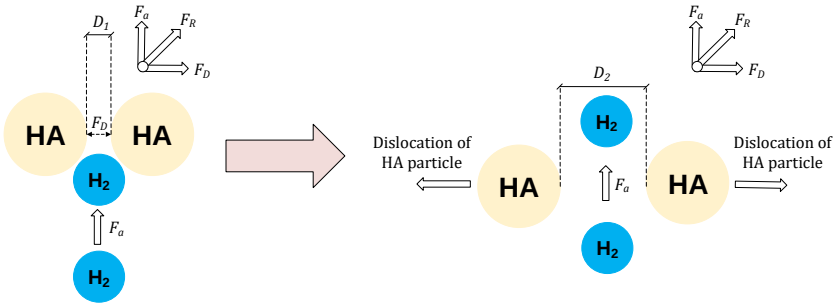

(b)

Figure 6 Schematic diagram of the behavior of hydrogen gas formed on the particle size of hydroxyapatite

H_2 gas in the bulk solution causes an outward pushing force through the cracks of the hydroxyapatite NPs, causing the electrolytic synthesized particles to have a smaller size. The white powder synthesized by electrolysis at a potential of 6 Volt has a more heterogeneous particle distribution than the particles synthesized at 4 and 5 Volts. Meanwhile, the distribution of commercial hydroxyapatite particles tends to have a large distribution range. This is due to particle agglomeration, which causes a larger range of particle size distribution.

3.4. The Surface Area of the Synthesized Particles

The surface area of the HA NPs showed that the hydroxyapatite particles synthesized at the 4 Volt potential had a smaller surface area than those synthesized at the 5 Volt and 6 Volt potentials, which had almost the same surface area. The particles synthesized with low potential have better porosity than those synthesized at high potential. This is because the pores structure of HA NPs synthesized at the high potential has a tendency to collapse, so that the pore area tends to be small (Hong *et al.*, 2013). Whereas commercial hydroxyapatite particles have a smaller surface area than synthetic hydroxyapatite at a potential of 4 Volts and greater than synthetic hydroxyapatite at 5 Volts and 6 Volts.

Table 1 The surface area of the synthesized particles by electrolysis and commercial hydroxyapatite

Electrolysis Potential (Volt)	Surface area (m^2/gram)
4	417.22
5	304.247
6	303.419
HA commercial	355.779

4. Conclusions

Synthesis of pure hydroxyapatite (100% hydroxyapatite) by electrolysis was successfully carried out at a potential of 5 volts. The OH^- ion, which comes from the H_2O reduction process at the cathode, plays a critical role in the formation of brushite forming hydroxyapatite. The hydroxyapatite, synthesized at a potential of 4 volts, had the smallest particle size (442.4 nm) with the largest particle surface area (417.22 m^2/gram). Further research needs to examine the effect of the synthesis time of HA NPs, which is longer than 6 hours with a voltage of 4 Volts to determine the most effective time variable in the synthesis of hydroxyapatite.

Acknowledgments

This work was supported by HPP (HIBAH PENELITI PEMULA) 2020 through grant Number 436.74/UN10.C10/PN/2020.

References

Banerjee, A., Bandyopadhyay, A., Bose, S., 2007. Hydroxyapaptite nanopowders: synthesis, densification and cell materials interaction. *Materials Science and Engineering: C*, Volume 27(4), pp. 729–735

Chang, M.C., Tanaka, J., 2002. FT-IR study for hydroxyapatite/collagen nanocomposite cross-linked by glutaraldehyde. *Biomaterials,* Volume 23(24), pp. 4811–4818

Córdova-Udaeta, M., Kim, Y., Yasukawa, K., Kato, Y., Fujita, T., Dodbiba, G., 2021. Study on the synthesis of hydroxyapatite under highly alkaline conditions. *Industrial & Engineering Chemistry Research,* Volume 60(11), pp. 4385–4396

Corona-Gomez, J., Chen, X., Yang Q., 2016. Effect of nanoparticle incorporation and surface coating on mechanical properties of bone scaffold: a brief review. *Journal of Functional Biomaterials,* Volume 7(3), p. 18

Djosic, M.S., Miskovic-Stankovic, V.B., Kacarevic-Popovic, Z.M., Jokic, B.M., Bibic, N., Mitric, M., Milonjic, S.K., 2009. Electrochemical synthesis of nanosized monetite powder and its electrophoretic deposition on titanium. *Colloids and Surfaces A: Physicochemical and Engineering Aspects,* Volume 341(1), pp. 110–117

Dorozhkin, S.V., 2010. *Bioceramics of calcium orthophosphates*. Biomaterials, Volume 31(7), pp. 1465–1485

Fathi, M.H., Hanifi, A., 2007. Evaluation and chracterization of nanostructure hydroxyapatie powder prepared by simple sol–gel method. *Materials Letters,* Volume 61(18), pp. 3978–3983

Hong, X.T., Wu, X.H., Mo, M.Y., Luo, Z. P., HUI, K., Chen, H.Y., Zhang, Q.Y., 2013. Synthesis and electrochemical capacitive performances of novel hierarchically micro-meso-structured porous carbons fabricated using Microporous rod-like hydroxyapatites as a template. *Acta Physico-Chimica Sinica*, Volume 29(2), pp. 298–304

Kamitakahara, M.R., Imai, Ioku, K., 2013. Preparation and evaluation of spherical ca-deficient hydroxyapatite granules with controlled surface microstructure as drug carriers. *Materials Science and Engineering: C,* Volume 33(4), pp. 2446–2450

Kim, W.S., Kim, W.S., Hirasawa, I., 2002. Changes in crystalline properties of nanosized hydroxyapatite powders prepared by low-temperature reactive crystallization. *Journal of chemical engineering of Japan,* Volume 35(11), pp. 1203–1210

Lin, D.J., Hung F.Y., Lee H.P., Yeh M.L., 2017. Development of a novel degradation-controlled magnesium-based regeneration membrane for future guided bone regeneration (GBR) therapy. *Metals,* Volume 7(11), p. 481

Martins, M., Santos, C., Almeida, M., Costa M., 2008. Hydroxyapatite micro and nanoparticles: nucleation and growth mechanism in the presence of citrate species. *Journal of Colloid and Interface Science,* Volume 318(2), pp. 210–216

Montero, M.L., Saenz, A., Rodriguez, J., Arenas, J., Castano, V.M., 2006. Electro-chemical synthesis of nanoized hydroxyapatite. *Journal of materials science,* Volume 41(7), pp. 2141–2144

Nasiri-Tabrizi, B., Honarmandi, P., Ebrahimi-Kahrizsangi, R., Honarmandi, P., 2009. Synthesis of nanosize single-crystal hydroxyapatite via mechanochemical method. *Materials Letters*, Volume 63(5), pp. 543–546

Nur, A., Setyawan, H., Widjaja, A., Lenggoro, I. W., 2014. Electrochemical processes for the formation of hydroxyapatite powders. *Bulletin of Chemical Reaction Engineering & Catalysis,* Volume 9(3), pp. 168–175

Panda, S., Biswas, C.K., Paul, S., 2021. A comprehensive review on the preparation and application of calcium hydroxyapatite: a special focus on atomic doping methods for bone tissue engineering. *Ceramics International*, Volume 47(20), pp. 28122–28144

Pietrzykowska, E., Romelczyk-Baishya, B., Chodara, A., Koltsov, I., Smogór, H., Mizeracki, J., Łojkowski, W., 2021. Microstructure and mechanical properties of inverse nanocomposite made from polylactide and hydroxyapatite nanoparticles. *Materials,* Volume 15(1), p. 184

Rezwan, K., Chen, Q.Z., Blaker, J.J., Boccacini, A.R., 2006. Biodegradable and bioactive porous polymer/inorganic composite scaffolds for bone tissue engineering. *Bomaterias*. Volume 27(18), pp. 3413–3431

Suchanek, W., Yoshimura, M., 1998. Processing and properties of hydroxyapatite-based biomaterials for use as hard tissue replacement implants*. Journal of Materials Research,* Volume 13(1), pp. 94–117

Tomozawa, M., Hiromoto, S., 2011. Microstructure of hydroxyapatite- and octacalcium phosphate-coatings formed on magnesium by a hydrothermal treatment at various pH values. *Acta Materialia*, Volume 59(1), pp. 355–363

Tripathi, G., Basu, B., 2012. A Porous Hydroxyapatite Scaffold for Bone Tissue Engineering: Physico-Mechanical and Biological Evaluations. *Ceramics International*, Volume 38(1), pp. 341–349

Xin, R., Ren, F., Leng, Y., 2010. Synthesis and characterization of nano-crystalline calcium phosphates with EDTA assisted hydrothermal method. *Materials & Design,* Volume 31(4), pp. 1691–1694

Zhou, H., Lee, J., 2011. Nanoscale hydroxyapatite particles for bone tissue engineering. *Acta Biomaterialia,* Volume 7(7), pp. 2769–2781